



UHI Research Database pdf download summary

Novel species of the oomycete *Olpidiopsis* potentially threaten European red algal cultivation

Badis, Yacine; Klochkova, Tatyana A.; Strittmatter, Martina; Garvetto, Andrea; Murúa, Pedro; Sanderson, J. Craig; Kim, Gwang Hoon; Gachon, Claire M. M.

Published in:
Journal of Applied Phycology

Publication date:
2018

The re-use license for this item is:
CC BY-NC

The Document Version you have downloaded here is:
Peer reviewed version

The final published version is available direct from the publisher website at:
[10.1007/s10811-018-1641-9](https://doi.org/10.1007/s10811-018-1641-9)

[Link to author version on UHI Research Database](#)

Citation for published version (APA):

Badis, Y., Klochkova, T. A., Strittmatter, M., Garvetto, A., Murúa, P., Sanderson, J. C., Kim, G. H., & Gachon, C. M. M. (2018). Novel species of the oomycete *Olpidiopsis* potentially threaten European red algal cultivation. *Journal of Applied Phycology*. Advance online publication. <https://doi.org/10.1007/s10811-018-1641-9>

General rights

Copyright and moral rights for the publications made accessible in the UHI Research Database are retained by the authors and/or other copyright owners and it is a condition of accessing publications that users recognise and abide by the legal requirements associated with these rights:

- 1) Users may download and print one copy of any publication from the UHI Research Database for the purpose of private study or research.
- 2) You may not further distribute the material or use it for any profit-making activity or commercial gain
- 3) You may freely distribute the URL identifying the publication in the UHI Research Database

Take down policy

If you believe that this document breaches copyright please contact us at RO@uhi.ac.uk providing details; we will remove access to the work immediately and investigate your claim.

[Click here to view linked References](#)

1 **Novel species of the oomycete *Olpidiopsis* potentially threaten European red algal**
2 **cultivation**

3 Yacine Badis¹, Tatyana A. Klochkova², Martina Strittmatter^{1,3}, Andrea Garvetto¹, Pedro
4 Murúa^{1,4}, J. Craig Sanderson⁵, Gwang Hoon Kim⁶, Claire M.M. Gachon¹

5

6 ¹ The Scottish Association for Marine Science, Scottish Marine Institute, Oban, Argyll
7 PA37 1QA, United Kingdom; ² Kamchatka State Technical University, Petropavlovsk-
8 Kamchatsky, 683003, Russia; ³ Roscoff Biological Station, Place Georges Teissier, 29680
9 Roscoff, France; ⁴ Aberdeen Oomycete Laboratory, College of Life Sciences and
10 Medicine, University of Aberdeen, Foresterhill, Aberdeen, AB25 2ZD, United Kingdom;
11 ⁵Institute of Marine and Antarctic Studies, University of Tasmania, Hobart, Australia;
12 ⁶Department of Biology, Kongju National University, Kongju 32588, Korea

13

14 **Author for correspondence:** claire.gachon@sams.ac.uk

15 Tel: 0044 16 31 559 318

16

17 **Abstract**

18 The rapid growth of marine macroalgal cultivation amplifies the potential impacts of
19 seaweed diseases. Here, we combine microscopy and molecular analysis to describe
20 two novel European species, *Olpidiopsis palmariae* and *O. muelleri* spp. nov., that infect
21 the commercially important red algae *Palmaria* and *Porphyra*, respectively. A Scottish
22 variety of *Olpidiopsis porphyrae*, a devastating pathogen of *Pyropia* previously thought
23 to be restricted to Japanese seaweed farms, is also described as *O. porphyrae* var.
24 *scotiae*. In the light of their destructiveness in Asian farms, together with the global
25 expansion of algal cultivation and pertaining seed trade, *Olpidiopsis* pathogens should
26 be treated as a serious threat to the sustainability of red algal aquaculture. Our findings
27 call for the documentation of seaweed pathogens and the creation of an international
28 biosecurity framework to limit their spread.

29
30 **Keywords:**

31 Aquaculture, Algal Disease, Algal Parasite, Barcoding, Biosecurity, *Olpidiopsis*,
32 Oomycete, Rhodophyte.

33

34

35

36

37

38

39

40

41

42

43

44

45

46 **Introduction**

47 In the last 25 years, the production of *Pyropia* (formerly *Porphyra*), the alga extensively
48 used as sushi wrap in Asiatic cuisine, has more than tripled, mostly due to a rapid
49 expansion in China and Korea (FAO 2014, <http://www.fao.org>). Over the same period,
50 the production of seaweeds grown for their jellifying properties (carageenophytes and
51 agarophytes, including eucheumatoids and *Gracilaria*) has increased fifteen-fold. Many
52 more species, including *Palmaria palmata* (traditionally eaten as dulse in the UK) are
53 subjected to cultivation trials.

54 A recent analysis conducted in Korea showed that alongside the intensification of
55 production, disease management is a growing concern for farmers, and now contributes
56 up to half the running cost of a farm (Kim *et al.*, 2014); in the last three years, three new
57 species of pathogens infecting *Pyropia* have been described (Kim *et al.*, 2016; Klochkova
58 *et al.*, 2016b). This echoes a well-known pattern in agriculture and animal aquaculture,
59 whereby diseases are discovered when species first become cultivated in large scale
60 (e.g. for invertebrate aquaculture, Brasier, 2008; Stentiford *et al.*, 2011; Stentiford *et al.*,
61 2017). Therefore, the identification and characterisation of pathogens infecting algal
62 crops is becoming a research priority to underpin the sustainable development of the
63 industry (Cottier-Cook *et al.*, 2016). To ensure the conservation of native algal
64 biodiversity, it is also indispensable to understand the potential disease-mediated
65 interplay between crops and wild stocks (e.g. presence of pathogen reservoirs and wild-
66 crop cross-contamination, Loureiro *et al.*, 2015).

67 Amongst the most devastating pathogens of Asian *Pyropia* farms are the oomycetes
68 *Olpidiopsis porphyrae* and *O. pyropiae*, that are investigated in Japan and Korea (Arasaki,
69 1947 ; Arasaki, 1960; Park *et al.*, 2001; Ding *et al.*, 2005; Sekimoto *et al.*, 2008; Kim *et al.*,
70 2014; Klochkova *et al.*, 2016a; Kwak *et al.*, 2017). Additionally, *Olpidiopsis bostrychia*
71 was found infecting *Bostrychia moritziana*, a small red alga of the West Indian Ocean
72 mangroves (West *et al.*, 2006; Sekimoto *et al.*, 2009). Recently, records of *Olpidiopsis*
73 *feldmanni* and *Olpidiopsis heterosiphoniae* were also published (Fletcher *et al.*, 2015;
74 Klochkova *et al.*, 2017). To date, these marine endoparasites of red algae are the only

75 members of the *Olpidiopsis* genus characterised both molecularly and morphologically;
76 they form a monophyletic clade (commonly recognised as the order Olpidiopsidales),
77 most closely related to the Anisolpidiales and Haliphthorales (Gachon *et al.*, 2017).
78 Additional older records of holocarpic pathogens of red algae have been reviewed
79 elsewhere (Dick, 2001; Beakes *et al.*, 2014), but molecular information is lacking for all
80 of them. Likewise, and despite their destructiveness in Asia, there is no morphology-
81 based nor any molecular report of *Olpidiopsis* pathogens of red algae in Europe.

82 Taking into account the growing number of seaweed cultivation initiatives in European
83 waters, we set out to assess if the genus *Olpidiopsis* could represent a potential threat to
84 this developing aquaculture sector. Here, a modest sampling campaign of wild algal
85 populations and *Palmaria* cultivation facilities led us to the identification in Scotland of
86 two novel *Olpidiopsis* species, and of one species previously only reported in Japan
87 (Sekimoto *et al.*, 2008).

88 **Methods**

89 ***Biological material***

90 Details of all records of marine *Olpidiopsis* and their respective hosts are given in
91 Table S1, alongside with sampling location, GPS coordinates, host culture collection ID,
92 and Genbank sequence accession number (when applicable).

93 ***Palmaria palmata*** blades were collected from cultivation lines seeded in the wild (Isle
94 of Kerrera, Scotland, UK) in April 2015 and cultivated in 10.000 L fibreglass tanks for
95 two months (ambient light and temperature, continuous flow of seawater 7L/min).
96 Fertile *Palmaria* tetrasporophytes developed in those conditions, together with
97 epiphytic *Ectocarpus* filaments. *Olpidiopsis* Isolate 1 was encountered parasitizing
98 *Palmaria* tetraspores retained on epiphytic *Ectocarpus* filaments. Though stable
99 cultures were not established, the pathogen was successfully propagated into healthy
100 tetraspores as follows: healthy fertile tetrasporophytes were rinsed and maintained
101 overnight at 10°C in filtered sterile sea water, and a tetraspore suspension was obtained
102 by gentle centrifugation (2000g for 10min at 10°C). In an inoculation procedure
103 adapted from Strittmatter *et al.* (2013), a droplet of healthy tetraspore suspension was
104 placed in a 50 mm diameter, 20 mm-deep petri dish, covered with a 40- μ m mesh cell
105 strainer containing the infected material. The propagation of the parasite into the
106 tetraspores beneath the cell strainer was monitored by bright field microscopy and this
107 material was used for histological staining and DNA extraction.

108 ***Porphyra sp.*** blades infected with several *Olpidiopsis* parasites were collected from
109 various locations in Scotland (Table S1), namely the Shetland Islands (Isolate 2), Seil
110 Island (Isolate 4) and Oban.

111 ***Polysiphonia sp.*** specimens (infected with *Olpidiopsis* Isolate 3) were collected at low
112 tide (Clachan Bridge, Scotland, UK) and observed using conventional bright field
113 microscopy (Zeiss Observer Z1). Infected algal tips were dissected for subsequent DNA
114 extraction.

115 ***Histological staining***

116 Observations were made on fresh material, or samples fixed in 2% formaldehyde and
117 0,2% glutaraldehyde in phosphate buffered saline). Cell wall structures and nuclei were
118 stained with Calcofluor white and SYBR-Green, respectively (Gachon *et al.*, 2017).

119 ***DNA extraction sequencing and molecular phylogeny reconstruction***

120 DNA extraction of infected *Palmaria* tetraspore suspensions, infected *Porphyra* sp., and
121 infected *Polysiphonia* algal tips was performed according to Strittmatter *et al.* 2013.
122 Oomycete Cox1, Cox 2 and 18S markers were amplified (according to Gachon *et al.*,
123 2017) and individually subjected to phylogeny reconstruction with a representative
124 subset of published oomycete sequences. NCBI accession numbers of all sequences used
125 for phylogeny reconstruction are given in Table S2. Alignments were generated using
126 the MAFFT algorithm and manually corrected prior to phylogenetic analysis in MEGA v.
127 7 (Kumar *et al.*, 2016). Model tests were performed on each alignment prior to
128 maximum likelihood (ML) analysis to find the best substitution models. For the 18S
129 rRNA, Tamura-3-parameter was used (Tamura, 1992) with a discrete Gamma
130 distribution to model evolutionary rate differences among sites. The model by Le &
131 Gascuel was used with discrete gamma distribution for cox1 and cox2 markers (Le *et*
132 *al.*, 2008). The rate variation model allowed for some sites to be evolutionarily
133 invariable for the cox2 alignment. Maximum parsimony analysis was also performed on
134 all three datasets. Bootstrap re-sampling was set to 500 replicates. *Palmaria* and
135 *Polysiphonia* SSU markers were amplified using primers according to Saunders *et al.*
136 (2013), and default Neighbour Joining trees were generated in Geneious R6 (Fig. S7).

137 **Results and discussion**

138 ***A novel Olpidiopsis pathogen identified in Palmaria palmata cultivation facilities***

139 Isolate 1, hereafter identified as *O. palmariae* sp. nov., was discovered when monitoring
140 fertile *Palmaria palmata* tetrasporophytes grown in tanks (Fig. 1a,b and Fig. S1a). The
141 blades were colonised by brown filamentous epiphytes (*Ectocarpus* sp.) and displayed
142 an unusual punctuated aspect due to the germination of tetraspores before their release
143 (Fig S1b). Numerous free *Palmaria* tetraspores, as well as some young gametophytes
144 (Fig. 1b), were found entangled in the brown filamentous epiphytes. Most tetraspores
145 appeared dead and devoid of any cellular content, suggestive of an infection with an
146 intracellular holocarpic pathogen (arrows on Fig. 1b). Various developmental stages of

147 the parasite thallus were observed (Fig. 1c-h): young unwalled thalli in degrading red
148 algal cell structures (Fig. 1c), as well as older, granulous thalli filling entirely dead
149 *Palmaria* tetraspores (arrow on Fig. 1d). Each granular thallus developed an exit tube in
150 the course of spore differentiation (arrowhead on Fig. 1e). Some dead *Palmaria*
151 tetraspores contained mature pathogen sporangia with individualised encysted spores
152 (Fig. 1f) and multiple infections of the same tetraspore were frequent (Fig. 1g-h). Each
153 mature empty sporangium displayed one single exit tube of varying length (Fig. 1h). We
154 successfully propagated the pathogen by co-incubating infected material with freshly
155 released *Palmaria* tetraspores, enabling us to better observe its development (Fig. 2).
156 Uninfected tetraspores had a granulous content, with often an asymmetric repartition
157 of chloroplasts (Fig. 2a). We did not succeed in observing the penetration of the
158 pathogen into the red algal cell, and the earliest recognisable stage of infection was
159 characterised by a small refringent globule (ca. 2 μm in diameter) surrounded by a
160 spherical structure within the tetraspore cytosol (Fig. 2b). We assume that this perfectly
161 spherical shape is conferred by a prominent vacuole (arrow on Fig. 2c) that occupies
162 most of the thallus biovolume. Small vesicles (arrowheads on Fig. 2c) appeared at this
163 stage. Each thallus grew outwards very rapidly, as shown in a 21 min time course (Figs.
164 2d to 2f). During this period, increasing digestion of the red algal cell structures was
165 evident and absorption vesicles formed at the algal-pathogen interface, suggestive of
166 rapid incorporation of algal material by the parasite. The diameter of the absorption
167 vesicles increased with time, and they fused with the central globule (arrowheads on
168 Fig. 2e and 2f), suggesting that the latter is a storage structure. Once the tetraspore
169 content was fully assimilated, each thallus differentiated a cell wall (arrow on Fig. 2g)
170 and underwent radical ultrastructural changes. The refringent globule and the vacuole
171 both receded in size and became fragmented, leaving space for an increasingly dense
172 cytosol (Fig 2g-h). Just before sporogenesis, only dense cytoplasm was recognisable in
173 the once highly vacuolated thallus (Fig. 2i).

174 SYBR Green staining revealed that walled thalli are multinucleate syncytia (Fig. 3a):
175 Similar to recent observations conducted on the closely related pathogen *Anisolpidium*
176 *ectocarpii* (Gachon *et al.*, 2017), the nuclei of the younger stages were ca. 2.5 μm in
177 diameter with condensed peripheral material (arrowheads), whereas more mature
178 stages had dense compact nuclei ca. 1 μm in diameter (arrow). All nuclei within a

179 thallus were always at the same stage, therefore we assume that nuclear divisions are
180 synchronous, as is often the case in syncytial organisms. Multiple infections of the same
181 tetraspores were prevalent in our co-incubation experiment. In tetraspores containing
182 multiple parasites, SYBR Green and calcofluor white staining did not hint to sexual
183 fusion between antheridia and oogonia (Fig. 3b and c). Each sporangium produced one
184 exit tube. Calcofluor staining revealed that the length of the exit tubes varied widely
185 from 3 to ca. 20 μm (Fig. 3d, the inset shows the same infected spore in a different focal
186 plane). Remnants of encysted spores were observed on the surface of some host cells.
187 Those were 3 μm in diameter and had a thin, calcofluor-positive cell wall (Fig. 3e). Very
188 thin needle-like structures reminiscent of the penetration structure of *A. ectocarpii*
189 (Gachon *et al.*, 2017) were observed, through which spore content was injected into the
190 *Palmaria* host (arrowheads on fig 3e). It is unclear whether these infectious spores
191 encyst at the surface of the algal host directly following their release from the
192 sporangium, or if diplanetism might exist.

193 Comparable to other holocarpic oomycetes, the syncytium segmented to produce
194 spores (Fig. 2g-i). The dehiscence of one pathogen sporangium was observed, as well as
195 subsequent spore differentiation (Fig. 3f-h). Spores were about 3 μm in diameter and
196 assumed a light amoeboid movement inside the sporangium. Their release outside the
197 sporangium took a few minutes. As soon as the spores reached the outside medium,
198 they extended two straight flagella of unequal length within a minute or less (Fig. 3f and
199 g). During this process, the spores first assumed a triangular shape (Fig. 3f) and
200 progressively became spherical (h and i). The mature flagella were 3 and 8-10 μm ,
201 respectively, and bore a vesicle at their apex and tips (Fig. 3f-i, white arrowheads),
202 probably due to rapid reorganisation of their plasma membrane.

203 To the exception of individual cells of developing female gametophytes, no infection was
204 observed on any of the other *Palmaria* life stage available in culture (tetrasporophytes,
205 and embryos). In the absence of a stable supply of *Palmaria* tetraspores, this stage-
206 specificity of the parasite prevented its long-term laboratory cultivation.

207 Morphologically similar parasites were observed again several times in other
208 populations of *Palmaria palmata* grown in tanks, and on September 7th, 2015 on
209 individuals collected in Seil Island (Supplementary Table S1).

210 ***A novel Olpidiopsis parasite infecting both wild Porphyra and Polysiphonia***

211 Isolate 2, hereafter identified as *O. muelleri* sp. nov., stemmed from a female
212 gametophyte of *Porphyra* sp. harvested in the Shetland Islands due to its discoloured
213 margin (Fig. S1c,d). The infection was spatially restricted to the fertile margin where
214 red female gametes could still be found (Fig. 4a, arrowheads). The pathogen thalli were
215 granular and completely filled their host algal cell, which displayed an almost spherical
216 shape and altered brownish to greenish pigmentation (arrows). Each of the sporangia
217 developed a single and highly vacuolated exit tube (inset on Fig. 4b). Calcofluor white
218 staining of the same infected margin revealed a high density of infection (Fig. 4b, main
219 picture), and highlighted numerous *Olpidiopsis* empty sporangia with exit tubes of
220 varying length (ca. 20-80 μm). We did not observe any evidence of multiple infections of
221 the same algal cell. Numerous additional observations of *Olpidiopsis* parasitizing
222 *Porphyra* sp. were recorded from various blades collected in Oban and its surrounding
223 (Fig. S2) but they were not submitted to DNA barcoding.

224 Isolate 3, hereafter identified as *O. muelleri* var. *polysiphoniae*, was observed on
225 *Polysiphonia stricta*. The host alga displayed slightly curved growing tips (Fig. 4c), of
226 which several were infected (Fig. 4d). The parasite first developed as an apparently
227 unwallled granulous syncytium with granulous, greyish content which sometimes
228 completely filled the infected algal tip (Fig. 4d); spanning several algal cells, the cell wall
229 of which was still discernible (arrowheads on Fig. 4e). When infecting three-
230 dimensionally branched algal tips, the parasite thallus was lobed (arrow on e). Multiple
231 and perfectly spherical vacuoles could often be seen (Fig. 4f). The vacuolated thalli
232 displayed a clearly-defined wall (arrow). Additional smaller unwallled thalli could be
233 found in the same infected tip (arrowheads), suggesting multiple infections. Mature
234 parasite sporangia with individualized spores of ca. 5 μm in diameter were also
235 observed (Fig. 4g). Remains of excysted spore cell walls reminiscent of the honeycomb
236 structure typical of *Eurychasma* could be observed within empty sporangia (Fig. 4h),
237 and the latter typically displayed one or two short exit tubes (arrows in Fig. 4h). This
238 honeycomb structure is suggestive of sequential spore encystment/excystment, and
239 therefore of diplanetism. Spore release was not observed, and in the absence of
240 potential alternative hosts, the limited material prevented us from documenting further
241 the life cycle of this parasite.

242 ***A new variety of Asian Olpidiopsis parasite is present in Scotland***

243 Isolate 4, hereafter molecularly identified as *O. porphyrae* var. *scotiae*, was observed on
244 wild *Porphyra* blades collected from Easdale, Argyll, Scotland. Infected blades were
245 crinkled (Fig. S1e), resulting from localised necrotic lesions (arrows on Fig. S1f).
246 Diseased tissue revealed patches of infected host cells (Fig. 5a and higher magnification
247 on Fig. 5b). *Porphyra* cells containing pre-mature parasite thalli appeared light pink due
248 to degradation of algal pigments (dark arrows). The parasite thallus ultimately filled the
249 host cell, where remaining greenish algal material was compacted at the periphery
250 (dark arrowheads). The centre of infected patches usually displayed collapsed dead
251 cells of *Porphyra* (double arrowheads). Multiple infections of the same host cell were
252 frequently observed (Fig. 5c). In such multiple infections, calcofluor staining of the
253 parasite cell wall did not reveal any thallus fusion (inset in Fig. 5c), although further
254 ultrastructural work is needed to ascertain this result. Neighbouring dead collapsed
255 *Porphyra* cells (double arrowheads in Fig. 5c) were also calcofluor-positive, thus
256 revealing empty parasite sporangia. All empty sporangia observed displayed single exit
257 tubes of varying length (ca. 5-30 μm). SYBR-Green staining revealed fully grown
258 syncytial sporangia containing numerous nuclei (Fig. 5d). The number of nuclei (and
259 thus of infectious propagules) seemingly depended on the overall size of differentiating
260 sporangia, although no precise quantification was attempted. Diseased material was
261 incubated with fresh spores released by the same blade, leading to the observation of
262 successful spore infections (Fig. 5e).

263 **Molecular phylogeny unveils two novel *Olpidiopsis* species and unknown varieties** 264 **of Asian *Olpidiopsis* strains**

265 18S sequences were obtained for all four isolates described above. We were also
266 successful in obtaining a Cox2 sequence for Isolates 2 and 4 and a Cox1 sequence for
267 Isolate 4. All sequences generated in this study were submitted to Genbank (Table S1)
268 and used for Maximum Likelihood and Maximum Parsimony tree reconstruction (Fig. 6
269 and Fig. S3). All markers consistently grouped our four isolates with the known marine
270 *Olpidiopsis* parasitizing red algae, within a single clade (red arrow on Fig. 6 and Fig. S3),
271 most closely related to *Haliphthoros*, *Halocrusticida* and *Halodaphnea* (Haliphthorales).
272 Though the bootstrap values are mediocre, our 18S data further suggest that marine
273 *Olpidiopsis* species are split in three distinct clades, that we hereafter refer to as the

274 “*bostrychiae*”, “*pyropiae*” and “*porphyrae*” lineages. The parasite of *P. palmata* (Isolate 1)
275 was most closely related to *O. porphyrae*, with 98.8% identity on exons of the 18S
276 sequence. Its unique host, zoospore differentiation and 18S sequence set it aside from *O.*
277 *porphyrae* and we therefore propose to name it *Olpidiopsis palmariae* sp. nov. The 18S
278 sequence obtained for Isolate 2 was closest to *O. bostrychiae* (97% identity,
279 AB363063.1) while the amino acid Cox2 sequence formed a long branch clustered with
280 *O. porphyrae* (85% identity versus 72% identity with *O. bostrychiae*, Fig. S5). Therefore,
281 we conclude that isolate 2 is a novel species that we name *Olpidiopsis muelleri* sp. nov.
282 While no Cox2 sequence was obtained for the *Polysiphonia* parasite Isolate 3, its 18S
283 sequence was 100% identical to *O. muelleri* (Isolate 2). In contrast to all members of the
284 “*bostrychiae*” and “*porphyrae*” lineages, Isolate 3 forms honeycomb structures strongly
285 suggestive of diplanetism. This specific phenology argues against Isolate 3 being
286 conspecific with any of the *Olpidiopsis* already described, especially *O. muelleri*.
287 However, we were unable to observe zoospore behaviour on *O. muelleri* (Isolate 2).
288 Therefore, our conservative interpretation is to consider Isolates 2 and 3 as conspecific
289 until more molecular or morphological evidence is obtained. In order to take into
290 account its different host and phenology compared to Isolate 2, we refer to Isolate 3 as
291 *O. muelleri* var. *polysiphoniae*. Finally, the 18S and Cox1 sequences of Isolate 4 were
292 100% identical to *O. porphyrae*. Its virtually translated Cox2 sequence was 99.4%
293 identical to *O. porphyrae* (one substitution over 180 amino acid residues). Introns were
294 also detected in the 18S sequence, some of which were conserved with *O. porphyrae*
295 and/or with *O. porphyrae* var. *koreanae* (Fig. S6). Taking into account its original intron-
296 exon structure, a feature already used to erect the Korean variety *O. porphyrae* var.
297 *koreanae* (Kwak *et al.*, 2017), we refer to this isolate as *O. porphyrae* var. *scotiae*.

298

299 **Conclusion**

300 Here we describe two pathogens, *Olpidiopsis palmariae* and *O. muelleri* spp. nov. and
301 report two novel varieties *O. muelleri* var. *polysiphoniae* and *O. porphyrae* var. *scotiae*
302 from Scotland. In the light of our modest sampling efforts, this work illustrates the
303 widespread occurrence of undocumented *Olpidiopsis* species infecting both wild and
304 cultivated algae in Europe. The destructiveness of *O. pyropiae* and *O. porphyrae* in Asia
305 demonstrates the risk posed by these oomycete pathogens for the red seaweed industry
306 (Ding and Ma, 2005; Kim *et al.*, 2014; Kwak *et al.*, 2017). Accordingly, disease

307 management has become an integral part of farm design and operation in Asia; most
308 recently, insurance schemes have been set-up to protect farmers against worsening
309 crop losses (Cottier-Cook *et al.*, 2016). Our repeated observations of *O. palmariae* in
310 cultivation facilities in Scotland, combined with multiple accounts by growers of
311 hitherto unexplained seeding failures, highlights the real possibility of yield-limiting
312 epidemic outbreaks in the nascent Western aquaculture industry, and echoes repeated
313 reports of *Petersenia* diseases in Canadian *Chondrus* production facilities (Craigie *et al.*,
314 1996 and refs therein). This first European report of an *Olpidiopsis* species which is
315 already known to be highly destructive in Asia, opens the question of the potential
316 economic impact that non-native pathogens could have on Asian crops, especially if they
317 were introduced as a result of unregulated seed movements. Taken together, our
318 findings call for a much more systematic documentation of seaweed pathogens and the
319 creation of an international biosecurity framework to monitor and limit their spread.

320 **Taxonomy**

321

322 ***Olpidiopsis palmariae* Y. Badis & C.M.M. Gachon sp. nov.**

323 Vegetative thalli endobiotic, spherical, 2.3–4 µm in diameter when young, 10–50 µm
324 before cell-wall thickening and zoospore cleavage; completely filling host cell at
325 maturity, single discharge tube of variable length (3.5 to 30 µm) protruding from the
326 algal tetraspore; Multiple infections frequent (typically 2-5 thalli in one host cell in
327 holotype material), resulting in angular sporangia after cell wall thickening; zoospores
328 maturing outside of zoosporangium, triangular to spherical at maturity, 2.5–3.5 µm in
329 diameter, laterally biflagellate; flagella perpendicular and of unequal length (3 and 8-10
330 µm, respectively), differentiating upon discharge of the spores from the sporangium and
331 bearing at least temporarily submicrometric vesicles at their apical extremity; resting
332 spores unknown; obligate endoparasite in *Palmaria palmata* (Rhodophyceae). Only
333 observed infecting tetraspores or very young (2-8 cells) gametophytes.

334 HOLOTYPE: MuseumID (Population of infected *Palmaria* tetraspores in
335 formaldehyde/glutaraldehyde TEM buffer), National History Museum, London (NHM).

336 Type specimens are specific of *Palmaria palmata* tetraspores.

337 ILLUSTRATION WITH ANALYSIS: Fig. 2

338 PARATYPES: MuseumID (resin-embedded EM specimen), National History Museum,
339 London (NHM).

340 TYPE LOCALITY: Kerrera Island, Oban, Scotland, United Kingdom.

341 TYPE CULTURE: None

342 ETYMOLOGY: Named after its algal host.

343 GenBank accession number: KY403502 (18S)

344

345 ***Olpidiopsis muelleri* Y. Badis & C.M.M. Gachon sp. nov.**

346 Vegetative thalli endobiotic, spherical, 10–50 µm in diameter and zoospore cleavage;
347 completely filling host cell at maturity; single vacuolated discharge tube (variable
348 length, 20 to 80 µm) protruding from the host algal cortex at maturity; zoospores not
349 observed; obligate endoparasite in *Porphyra* sp. gametophyte.

350 HOLOTYPE: MuseumID (Fragment Infected *Porphyra* blade (Fig. S1.c-d) in
351 formaldehyde/glutaraldehyde TEM buffer), National History Museum, London (NHM).

352 ILLUSTRATIONS WITH ANALYSIS: Fig 4a-b.

353 ISOTYPES: MuseumID (Additional fragment of the same infected *Porphyra* blade, Fig.
354 S1.c-d) in formaldehyde/glutaraldehyde TEM buffer), National History Museum,
355 London (NHM).

356 TYPE LOCALITY: Lunna, Shetland Islands, Scotland, United Kingdom. (60°24'; -1°07')

357 TYPE CULTURE: None.

358 ETYMOLOGY: Named after Professor Dieter. G. Mueller, in recognition of his pioneering
359 contribution to the study and laboratory cultivation of marine oomycetes.

360 Genbank accession numbers: KY403503 (18S) and KY403508 (Cox2)

361

362

363 ***Olpidiopsis muelleri* var. *polysiphoniae* Y. Badis & C.M.M. Gachon var. nov.**

364 Vegetative thalli endobiotic, elongated, 10–50 µm, restricted to algal tips, completely
365 filling several adjacent cells, causing slight hypertrophy of algal tips, possibly lobed in
366 bifurcated algal tips; thalli naked in early stages, walled and vacuolated in later stages;
367 1-2 short discharge tubes (5 µm) protruding from the host algal cortex at maturity;
368 Zoospores sub-spherical, 3 to 5 µm in diameter, diplanetic, maturing and encysting in
369 sporangium. Remains of excysted spore cell walls visible in empty sporangium, forming
370 an irregular honeycomb structure. Obligate endoparasite in apices of *Polysiphonia* sp.

371 ICONOTYPE: Fig. 4c-h
372 TYPE LOCALITY: Atlantic Bridge, Seil Island, Scotland, United Kingdom. (56°17'; -5°58')
373 TYPE CULTURE: None.
374 ETYMOLOGY: Named after *Olpidiopsis muelleri*, on the basis of its identical 18S
375 sequence, and the specific host of this isolate.
376 Genbank accession number: KY403501 (18S).

377

378 ***Olpidiopsis porphyrae* var. *scotiae* Y. Badis, G.H. Kim, T.A. Klochkova & C.M.M.**

379 ***Gachon* var. nov.**

380 Vegetative thalli endobiotic, spherical to ellipsoidal, 2.5–6 µm in diameter when young,
381 12–30 µm in size when mature before spore cleavage; with 1 discharge tube protruding
382 from the host algal cortex at maturity. One sporangium contains 4–32 (rarely 64) spores
383 at maturity, depending on host algal species. Zoospores spherical to reniform, 2.2–3.5
384 µm in size, biflagellate, motile, maturing in sporangium; two flagella of unequal length,
385 inserted sub-apically, positioned at 45° angle. Dormant cysts spherical to ovoid, non-
386 motile, without flagella, maturing in sporangium. Armored resting spores absent; sexual
387 reproduction absent. Obligate endoparasite in *Porphyra* and *Pyropia* spp. 18S rRNA
388 gene sequence contains 5 group I introns.

389 COLLECTION: Oban, Scotland; May 2016; by Kim G.H.

390 ICONOTYPE: Fig. 5

391 TYPE LOCALITY: Seil Island, Scotland, United Kingdom. (56°17'; -5°39')

392 ETYMOLOGY: Named after *Olpidiopsis porphyrae*, and the type locality of this isolate.

393 GenBank accession number: KY403504 (18S), KY403506 (cox1), KY403505 (cox2).

394

395 **Acknowledgements**

396 This work was supported through the UK NERC IOF Pump-priming + scheme
397 (NE/L013223/1 – Y.B./C.M.M.G.), the European Union's Horizon 2020 research and
398 innovation (ALFF No 642575 – A.G./C.M.M.G; EMBRIC No 654008 – C.M.M.G.), the
399 Genomia fund (HERDIR – M.S), and a MASTS Visiting Fellowship Scheme (J.C.S.). P.M.
400 was funded by Conicyt (BecasChile N°72130422) for PhD studies at the University of
401 Aberdeen, and by the NERCIOF Pump-priming (scheme NE/L013223/1) for activities at
402 the Scottish Association for Marine Sciences. This work was partially supported by a
403 National Research Foundation of Korea Grant (NRF-2015M1A5A1041804) funded to

404 G.H.K. We are also grateful Duncan Smallman and Philip Kerrison for providing
405 *Palmaria* specimens.

406

407 **Author Contributions**

408 CMMG, GHK, YB and TAK designed the experiments; CMMG and GHK supervised the
409 research; YB, CMMG, GHK and JCS conducted the fieldwork; YB, TAK, MS, AG and PM
410 conducted the laboratory work YB and CMMG wrote the manuscript with contributions
411 from all co- authors. All authors gave final approval for publication.

412

413 **References**

414 Arasaki S. 1947. Studies on the rot of *Porphyra tenera* by a *Pythium*. *J. Jap Soc. Fish.*, 74-90.

415

416 Arasaki S. 1960. A chytridean parasite on the *Porphyra*. *Bull. Jap. Soc. Sci. Fish.*, 543-8.

417

418 Beakes G. W., Honda D. & Thines M. 2014. Systematics of the Straminipila: Labyrinthulomycota,
419 Hyphochytriomycota, and Oomycota. *In: MCLAUGHLIN, D. J. & SPATAFORA, J. W. (eds.)*
420 *Systematics and Evolution 2d edition The Mycota VII part A.*

421

422 Brasier C. M. 2008. The biosecurity threat to the UK and global environment from international
423 trade in plants. *Plant Pathology*, 57, 792-808.

424

425 Cottier-Cook E. J., Nagabhatla N., Badis Y., Campbell M. L., Chopin T., Dai W., *et al.* 2016.
426 Safeguarding the future of the global seaweed aquaculture industry. *United Nations University*
427 *(INWEH) and Scottish Association for Marine Science Policy Brief. ISBN 978-92-808-6080-1.*

428

429 Craigie J. S. & Correa J. A. 1996. Etiology of infectious diseases in cultivated *Chondrus crispus*
430 (*Gigartinales*, *Rhodophyta*). *Hydrobiologia*, 326, 97-104.

431

432 Dick M. W. 2001. Straminipilous fungi: systematics of the peronosporomycetes, including
433 accounts of the marine straminipilous protists, the plasmodiophorids, and similar organisms.,
434 pp 362-366.

435

436 Ding H. & Ma J. 2005. Simultaneous infection by red rot and chytrid diseases in *Porphyra*
437 *yezoensis* Ueda. *Journal of Applied Phycology*, 17, 51-56.

438

439 Fletcher K., Uljevic A., Tsirigoti A., Antolic B., Katsaros C., Nikolic V., *et al.* 2015. New record and
440 phylogenetic affinities of the oomycete *Olpidopsis feldmanni* infecting *Asparagopsis* sp.
441 (*Rhodophyta*). *Diseases of aquatic organisms*, 117, 45-57.

442

443 Gachon C. M., Strittmatter M., Badis Y., Fletcher K. I., Van West P. & Müller D. G. 2017. Pathogens
444 of brown algae: culture studies of *Anisolpidium ectocarpii* and *A. rosenvingei* reveal that the
445 *Anisolpidiales* are unflagellated oomycetes. *European Journal of Phycology*, 52, 133-148.

446
447 Kim G. H., Klochkova T. A., Lee D. J. & Im S. H. 2016. Chloroplast virus causes green-spot disease
448 in cultivated *Pyropia* of Korea. *Algal Research*, 17, 293-299.

449
450 Kim G. H., Moon K.-H., Kim J.-Y., Shim J. & Klochkova T. A. 2014. A revaluation of algal diseases in
451 Korean *Pyropia* (*Porphyra*) sea farms and their economic impact. *ALGAE*, 29, 249-265.

452
453 Klochkova T. A., Jung S. & Kim G. H. 2016a. Host range and salinity tolerance of *Pythium*
454 *porphyrae* may indicate its terrestrial origin. *Journal of Applied Phycology*, 1-9.

455
456 Klochkova T. A., Kwak M. S. & Kim G. H. 2017. A new endoparasite *Olpidiopsis heterosiphoniae*
457 sp. nov. that infects red algae in Korea. *Algal Research*.

458
459 Klochkova T. A., Shin Y. J., Moon K.-H., Motomura T. & Kim G. H. 2016b. New species of
460 unicellular obligate parasite, *Olpidiopsis pyropiae* sp. nov., that plagues *Pyropia* sea farms in
461 Korea. *Journal of Applied Phycology*, 28, 73-83.

462
463 Kumar S., Stecher G. & Tamura K. 2016. MEGA7: Molecular Evolutionary Genetics Analysis
464 Version 7.0 for Bigger Datasets. *Molecular biology and evolution*, 33, 1870-4.

465
466 Kwak M. S., Klochkova T. A., Jeong S. & Kim G. H. 2017. *Olpidiopsis porphyrae* var. *koreanae*, an
467 endemic endoparasite infecting cultivated *Pyropia yezoensis* in Korea. *Journal of Applied*
468 *Phycology*.

469
470 Le S. Q. & Gascuel O. 2008. An improved general amino acid replacement matrix. *Molecular*
471 *biology and evolution*, 25, 1307-20.

472
473 Loureiro R., Gachon C. M. & Rebours C. 2015. Seaweed cultivation: potential and challenges of
474 crop domestication at an unprecedented pace. *The New phytologist*, 206, 489-92.

475
476 Park C. S., Kakinuma M. & Amano H. 2001. Detection and quantitative analysis of zoospores of
477 *Pythium porphyrae*, causative organism of red rot disease in *Porphyra*, by competitive PCR.
478 *Journal of Applied Phycology*, 13, 433-441.

479
480 Saunders G. W. & Moore T. 2013. [Review] Refinements for the amplification and sequencing of
481 red algal DNA barcode and RedToL phylogenetic markers: a summary of current primers,
482 profiles and strategies. *ALGAE*, 28, 31-43.

483
484 Sekimoto S., Klochkova T. A., West J. A., Beakes G. W. & Honda D. 2009. *Olpidiopsis bostrychiae*
485 sp. nov.: an endoparasitic oomycete that infects *Bostrychia* and other red algae (*Rhodophyta*).
486 *Phycologia*, 48, 460-472.

- 487
 488 Sekimoto S., Yokoo K., Kawamura Y. & Honda D. 2008. Taxonomy, molecular phylogeny, and
 489 ultrastructural morphology of *Olpidiopsis porphyrae* sp. nov. (Oomycetes, straminipiles), a
 490 unicellular obligate endoparasite of *Bangia* and *Porphyra* spp. (Bangiales, Rhodophyta).
 491 *Mycological research*, 112, 361-74.
- 492
 493 Stentiford G. D. & Lightner D. V. 2011. Cases of White Spot Disease (WSD) in European shrimp
 494 farms. *Aquaculture*, 319, 302-306.
- 495
 496 Stentiford G. D., Sritunyalucksana K., Flegel T. W., Williams B. A. P., Withyachumnarnkul B.,
 497 Itsathitphaisarn O., *et al.* 2017. New Paradigms to Help Solve the Global Aquaculture Disease
 498 Crisis. *PLoS Pathogens*, 13, e1006160.
- 499
 500 Strittmatter M., Gachon C. M., Muller D. G., Kleinteich J., Heesch S., Tsirigoti A., *et al.* 2013.
 501 Intracellular eukaryotic pathogens in brown macroalgae in the Eastern Mediterranean,
 502 including LSU rRNA data for the oomycete *Eurychasma dicksonii*. *Diseases of aquatic organisms*,
 503 104, 1-11.
- 504
 505 Tamura K. 1992. Estimation of the number of nucleotide substitutions when there are strong
 506 transition-transversion and G+C-content biases. *Molecular biology and evolution*, 9, 678-87.
- 507
 508 West J. A., Klochkova T. A., Kim G. H. & Loiseaux-de Goër S. 2006. *Olpidiopsis* sp., an oomycete
 509 from Madagascar that infects *Bostrychia* and other red algae: Host species susceptibility.
 510 *Phycological Research*, 54, 72-85.

511

512

513 **Figure Legends**

514 **Fig. 1** *Olpidiopsis palmariae* – Main description

515 **a.** Cultivated blade of *Palmaria palmata* with epiphytic tufts of *Ectocarpus* sp. (thick
 516 brown arrows); the rare whitish necrotic lesions (white arrow) do not seem related
 517 with the *Olpidiopsis* disease. **b.** Numerous tetraspores associated to *Ectocarpus* tufts, as
 518 well as some young gametophytes. Most tetraspores appear dead, following an infection
 519 with an intracellular holocarpic pathogen (arrows). Inset: mature sporangium within a
 520 young gametophyte that is still pigmented. **c-h.** Development stages of the pathogen. **c.**
 521 Two young unwalled thalli (arrows) inside a degrading tetraspore. **d.** Thick-walled
 522 granulous thallus (arrow), surrounded by two mature empty sporangia (arrowheads).
 523 **e.** Sporangium (arrow) containing differentiating spores; Note the long thin exit tube
 524 (arrowhead). **f.** Sporangium with individualised encysted spores; note the absence of

525 honeycomb-like structure. **g.** Multiple infections of the same tetraspore are frequent. **h.**
526 Two empty thick-wall sporangia with exit tubes of different length (arrowheads). Bars :
527 b. 20 μm ; c-h. 10 μm .

528 **Fig. 2** *Olpidiopsis palmariae* – Pathogen nutrition inside the tetraspore

529 **a.** Healthy tetraspore of *Palmaria palmata*. **b.** Earliest stages of infection, showing small
530 individual globules (ca. 2 μm in diameter) surrounded by a vacuole **c.** Spherical thalli
531 (arrow) are delimited by a vacuole and contain a refringent central globule and small
532 absorption vesicles (arrowheads). **d-f** Time course over 20 minutes, showing rapid
533 outward growth of each thallus (arrow); note the formation, growth of absorption
534 vesicles at the thallus periphery, followed by their fusion with the central globule
535 (arrowheads). **g-i.** Structural changes in differentiating sporangia: **g-h.** Pathogen cell
536 wall differentiation in fully assimilated tetraspores; note the angular cell walls
537 separating several pathogen thalli; the vacuole and the refringent globule then start
538 receding, progressively leading to the granulous aspect shown in h. **i.** Initiation of
539 cytoplasm segmentation during sporogenesis; the upper sporangium already
540 discharged zoospores. **Legend:** Thick arrow: individual thallus; Thin arrow: Pathogen
541 cell wall; V-shaped arrowhead: vacuole. Arrowhead: absorption vesicle and/or
542 refringent globule. All bars: 10 μm .

543 **Fig. 3** *Olpidiopsis palmariae* – Sporogenesis and infection structures

544 **a.** Sybr-Green staining reveals multinucleate thalli at different stages. A nucleolus is
545 visible on younger stages nuclei (arrowheads), whereas more mature stages have dense
546 compact nuclei (arrows). **b.** Sybr-Green (left) and calcofluor white staining (right) do
547 not hint to thallus fusion **c.** Similar conclusions as in a-b, on a different object. **d.**
548 Calcofluor staining of multiple sporangia showing variability in the length of the exit
549 tubes. Inset: same infected spore in a different focal plane. **e.** Calcofluor staining
550 showing the remains of encysted pathogen spores bearing thin injection needles
551 (arrowheads). All bars. **f-g.** Rapid differentiation of flagella in two freshly released
552 spores. The pictures were taken ca. 1 min apart from each other. **h-i.** Spherical spores
553 with fully mature, straight flagella of unequal length, seen from different angles. In all
554 pictures, the arrowhead points to the bulging membranar structure at the tip of each
555 flagellum. Bars: a-e. 10 μm ; f-i. 2 μm .

556

557 **Fig. 4** *Olpidiopsis muelleri* on *Porphyra* sp. and *Polysiphonia* sp.

558 **a.** Close-up of fertile *Porphyra* sp. blade margin showing cells infected by
559 intracellular parasites (dark arrows) and healthy female cells (arrowheads) **b.**
560 Highly infected region stained with Calcofluor white. Note the varying length of
561 exit tubes (up to 80 μm). Inset: Single vacuolated exit tube (arrow) produced by
562 a by mature sporangium (arrow). **c.** Healthy filament tips of *Polysiphonia stricta*
563 **d.** Unwalled intramatrical thallus in a filament tip of *P. stricta*; Note the tip
564 swelling when compared to c. **e.** Lobed shape of the parasite thallus (arrow)
565 invading several algal cells. Note the visible remnants of the host cell walls
566 (arrowheads). **f.** Spherical vacuoles can often be seen at late stages of infection.
567 Note the clearly-defined wall (arrow), whereas the smaller thalli to the top and
568 bottom right are unwalled (arrowheads). **g.** Encysted spores in mature
569 sporangium. **h.** Empty sporangium with two rather short exit tubes (arrows).
570 Note the remains of excysted spore cell walls forming a coarse honeycomb
571 structure. Bars: a, e-f, and inset in b. 20 μm ; b. 100 μm ; c-g. 50 μm ; h. 10 μm .

572 **Fig. 5** *Olpidiopsis porphyrae* var. *scotiae* on Scottish *Porphyra* sp.

573 **a-b.** Necrotic patch of infected *Porphyra* cells. Note the contrasting pigmentation of
574 infected cells, ranging from pinkish in earlier stages (arrows) to greenish in later stages
575 (arrowheads). Dead collapsed host cells are usually observed in the centre of each patch
576 (double arrowheads). **c.** Multiple infections of *Porphyra* cells were frequently observed.
577 Inset: Calcofluor staining of parasite cell wall did not reveal any thallus fusion; collapsed
578 dead *Porphyra* cells (double arrowheads) are calcofluor positive, revealing empty
579 pathogen sporangia. **d.** Syncytial mature sporangia revealed by SYBR-Green staining. **e.**
580 *Olpidiopsis* thallus (arrow) growing in *Porphyra* spore.

581 **Fig. 6** Molecular phylogeny of marine members of the *Olpidiopsis* genus

582 Maximum Likelihood inference of the phylogeny of all known *Olpidiopsis* 18S sequences
583 using 500 Bootstrap replicates. The tree features four additional environmental 18S
584 sequences (EF100276, EF100297, AY426928, AY789783) identified by blastn searches
585 against Genbank. The red arrow points to the single clade grouping all *Olpidiopsis* and

586 *Anisolpidium* sequences. The Bootstrap values are reflected by the diameter and colour
587 of each node. Scale: number of nucleotide substitutions per site

588

589 **Supporting Information**

590 **Fig. S1** Additional captions of infected host algae

591 **Fig. S2** Additional *Olpidiopsis* sp. observed on a *Porphyra* sp. blade in Oban

592 **Fig. S3** 18S Phylogenetic tree (Maximum Parsimony)

593 **Fig. S4** Cox1 Phylogenetic trees

594 **Fig. S5** Cox2 Phylogenetic Trees

595 **Fig. S6** Intron Content in *Olpidiopsis porphyrae* varieties

596 **Fig. S7** Molecular characterization of some red algal hosts identified in this study

597 **Table S1** Summary table of all known *Olpidiopsis* sequences, OTUs described in this study, as
598 well as selected bibliographical records

599 **Table S2** List of all Genbank accessions used for 18S, Cox1, and Cox2 phylogeny reconstruction

600

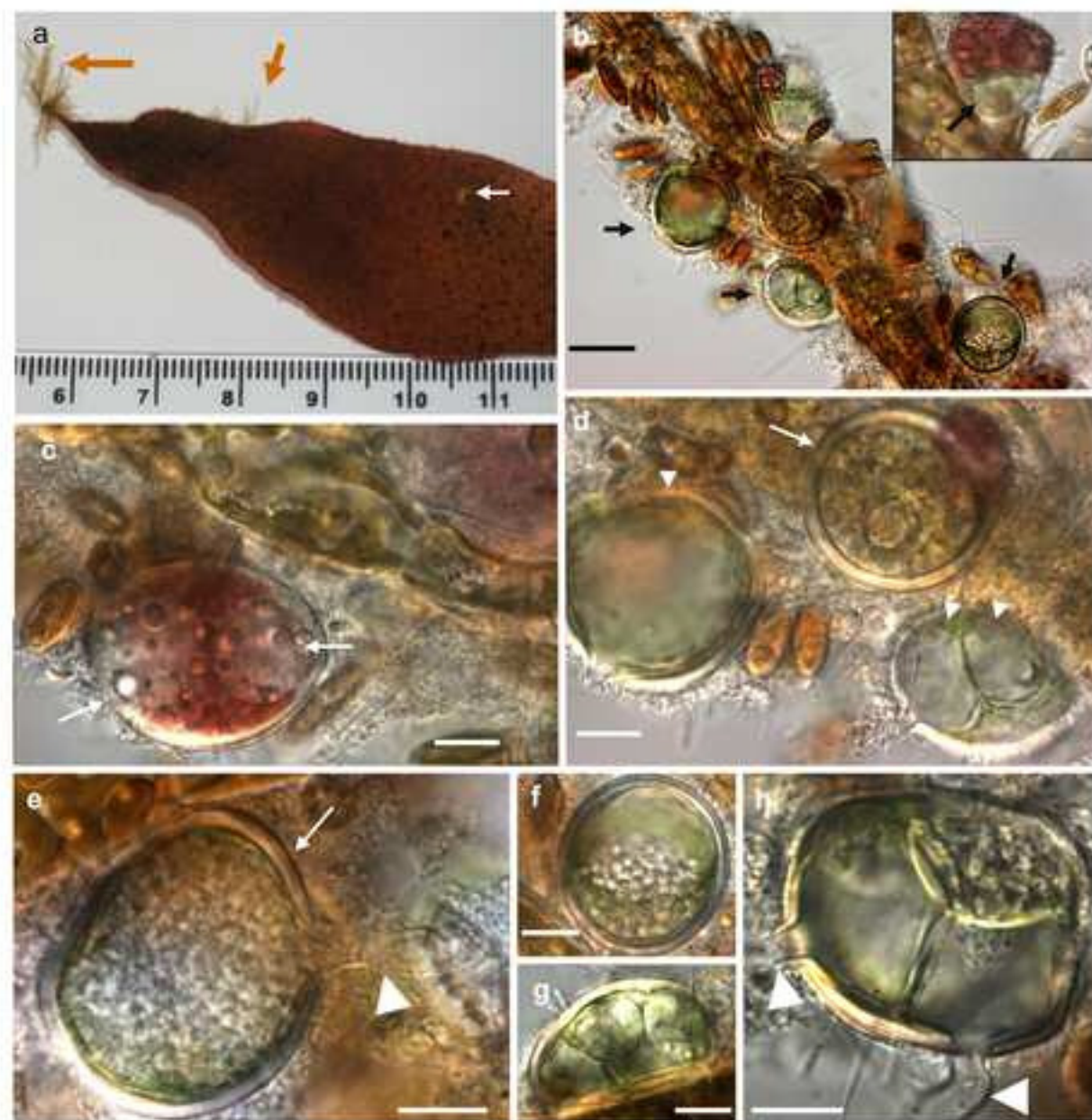


***Fig.1 Olpidiopsis palmariae* - Main description:**

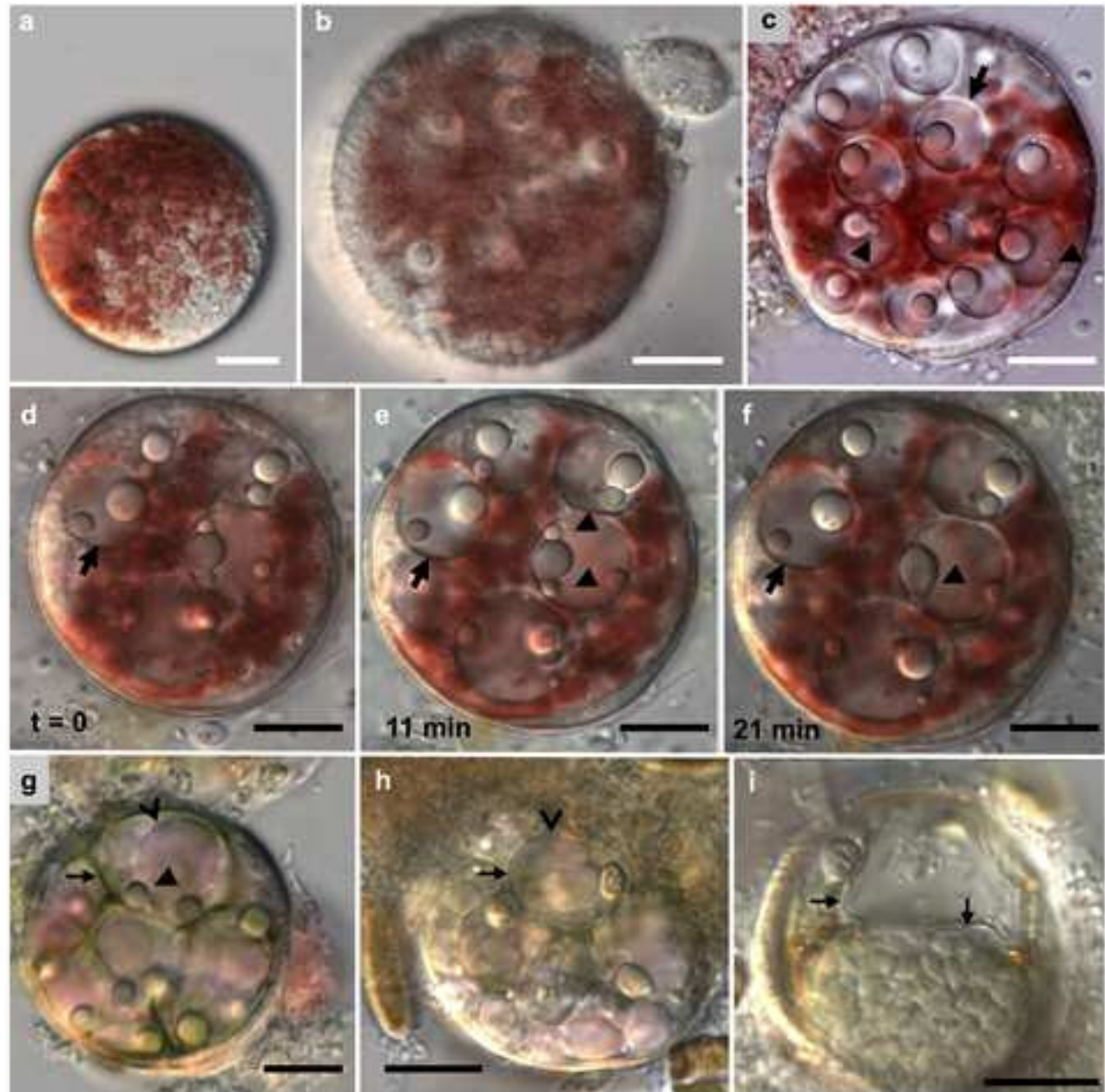


***Fig.2 Olpidiopsis palmariae* - Pathogen nutrition inside the tetraspore**

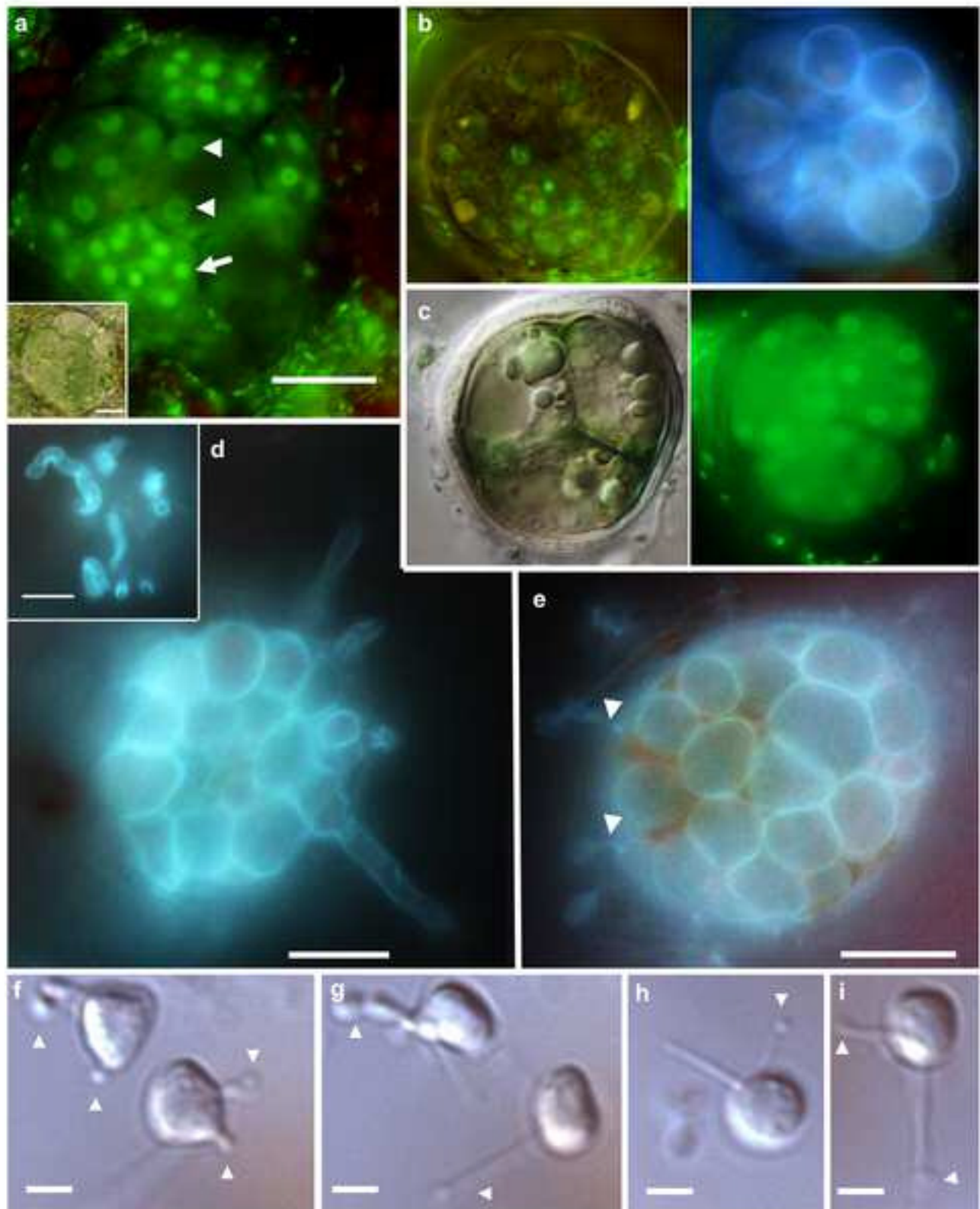


Fig.3. *Olpidiopsis palmariae* - sporogenesis and infection structures

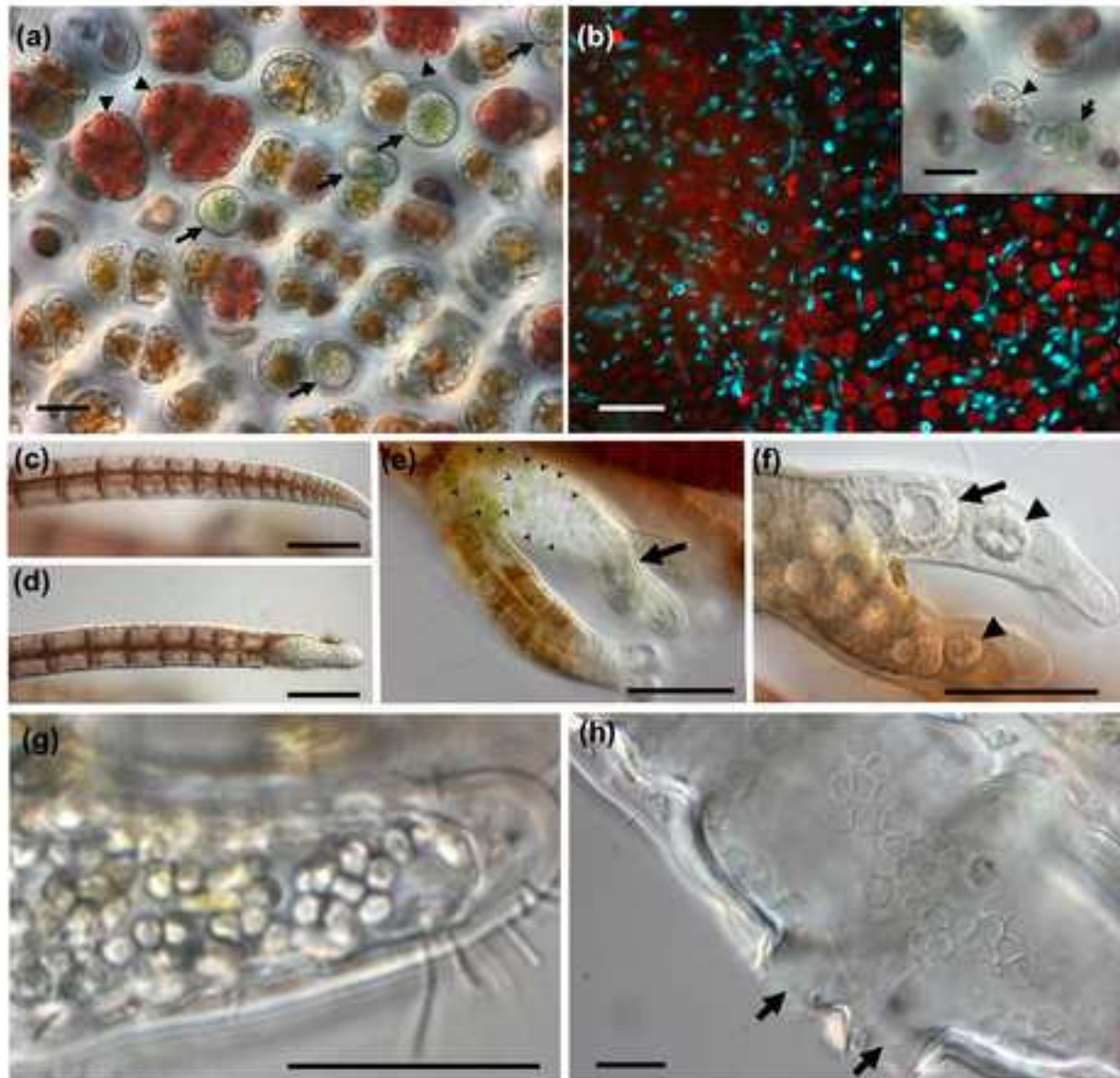


Fig. 4 *Olpidiopsis muelleri* sp. nov. on *Porphyra* sp. and *Polysiphonia* sp.

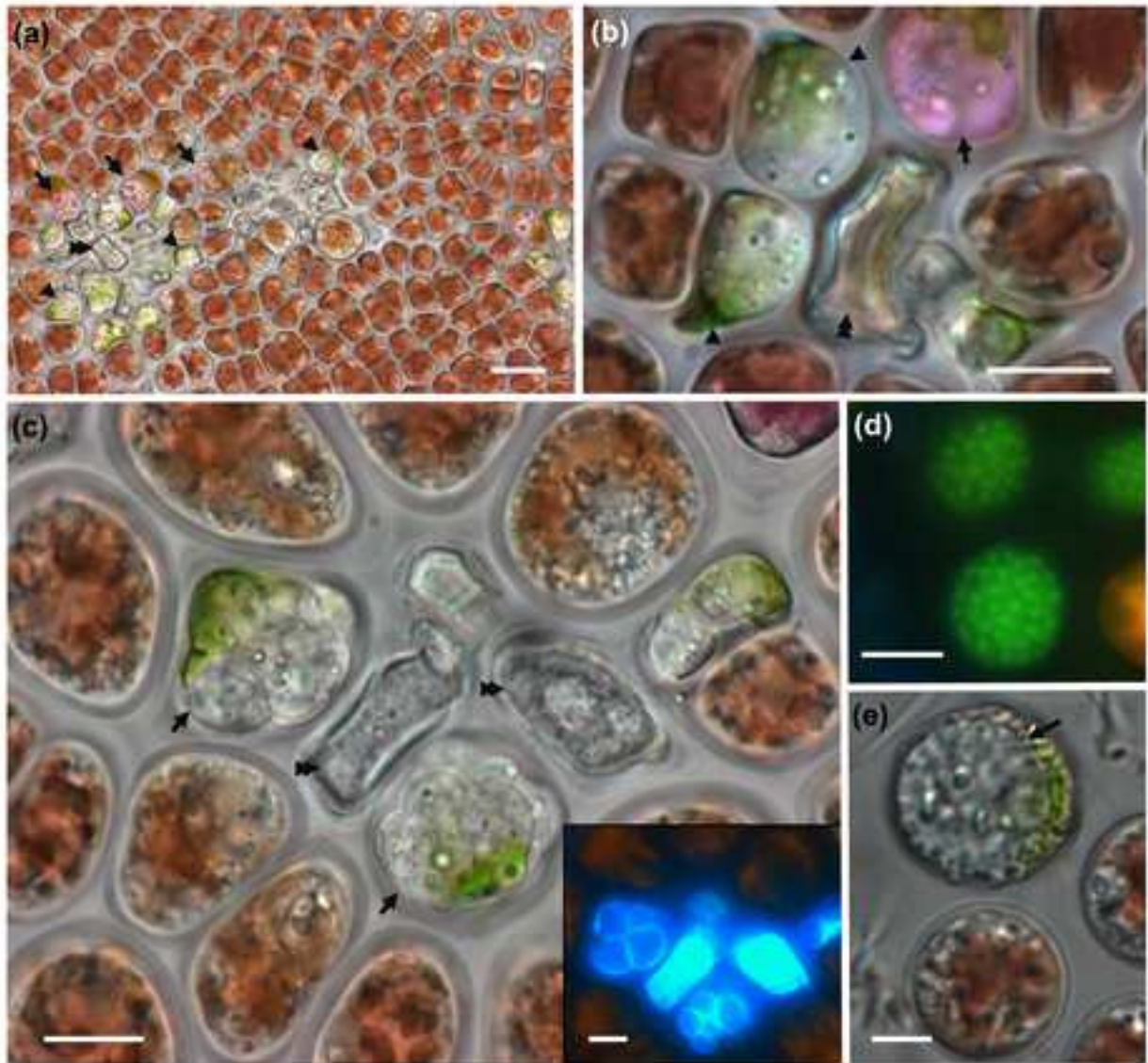


Fig. 5 *Olpidiopsis porphyrae* var. *scotiae* infecting *Porphyra* sp.

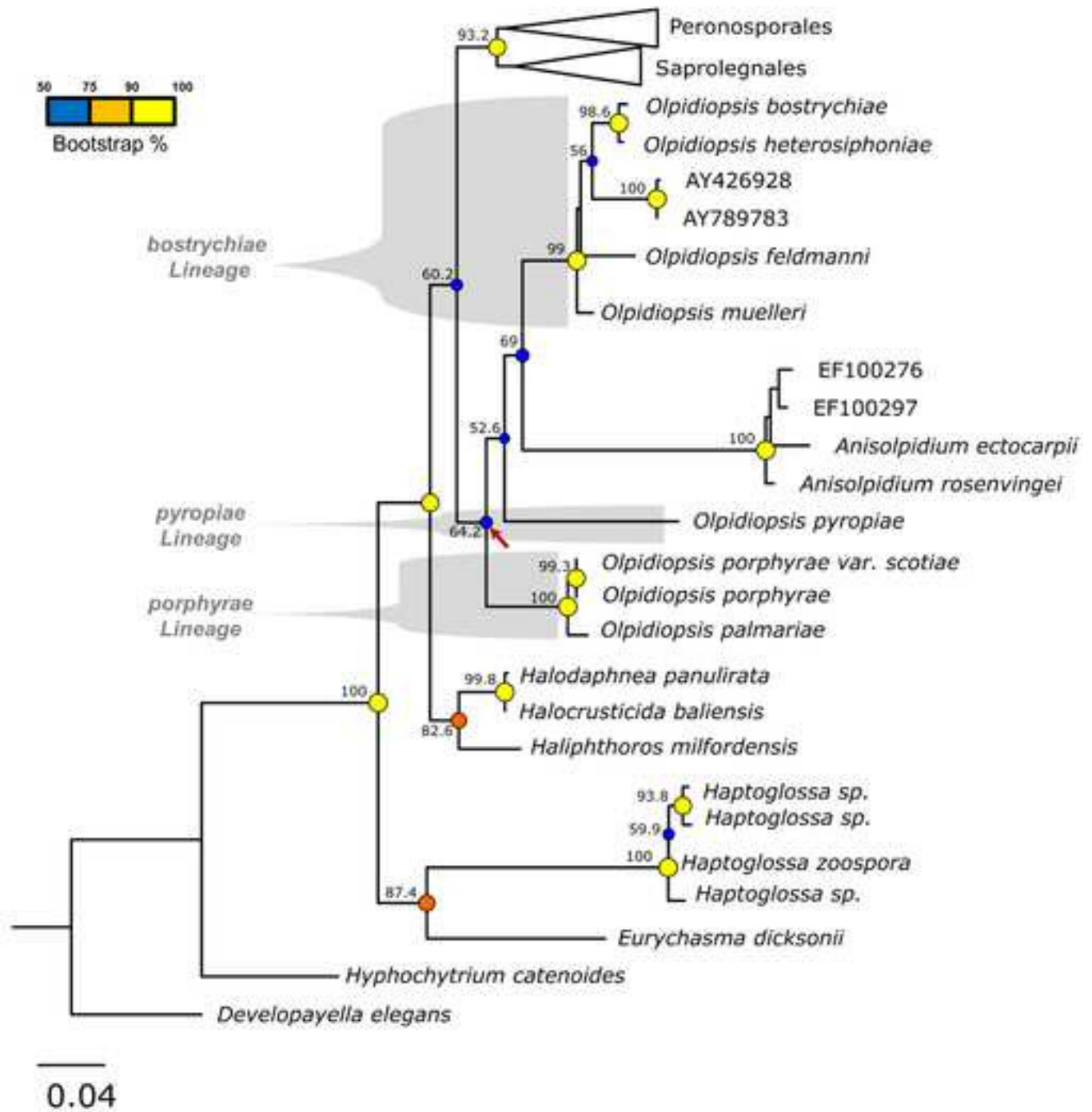


Fig. 6